

One-point statistics of the Lagrangian displacement field

Florent Leclercq,^{1,2,3,a)} Jens Jasche,⁴ and Benjamin Wandelt^{1,2,5,6}

¹⁾*Institut d’Astrophysique de Paris (IAP), UMR 7095, CNRS – UPMC Université Paris 6, Sorbonne Universités, 98bis boulevard Arago, F-75014 Paris, France*

²⁾*Institut Lagrange de Paris (ILP), Sorbonne Universités, 98bis boulevard Arago, F-75014 Paris, France*

³⁾*École polytechnique ParisTech, Route de Saclay, F-91128 Palaiseau, France*

⁴⁾*Excellence Cluster Universe, Technische Universität München, Boltzmannstrasse 2, D-85748 Garching, Germany*

⁵⁾*Department of Physics, University of Illinois at Urbana-Champaign, 1110 West Green Street, Urbana, IL 61801, USA*

⁶⁾*Department of Astronomy, University of Illinois at Urbana-Champaign, 1002 West Green Street, Urbana, IL 61801, USA*

(Dated: 12 November 2018)

This document is an addendum to “One-point remapping of Lagrangian perturbation theory in the mildly non-linear regime of cosmic structure formation” (Leclercq *et al.*, 2013).

The remapping procedure, described in section II of the main paper (Leclercq *et al.*, 2013), relies on the Eulerian density contrast. As noted by previous authors (see in particular Neyrinck, 2013), in the Lagrangian representation of the large-scale structure, it is natural to use the divergence of the displacement field ψ instead of the Eulerian density contrast δ . This addendum provides additional comments on the one-point statistics of ψ and comparatively analyzes key features of ψ and δ .

In the Lagrangian frame, the quantity of interest is not the position, but the displacement field $\Psi(\mathbf{q})$ which maps the initial comoving particle position \mathbf{q} to its final comoving Eulerian position \mathbf{x} (see e.g. Bouchet *et al.*, 1995 or Bernardeau *et al.*, 2002 for overviews),

$$\mathbf{x} \equiv \mathbf{q} + \Psi(\mathbf{q}). \quad (1)$$

It is important to note that, though $\Psi(\mathbf{q})$ is *a priori* a full three-dimensional vector field, it is curl-free up to second order in Lagrangian perturbation theory (appendix D in Bernardeau, 1994 or Bernardeau *et al.*, 2002 for a review). We did not consider contributions beyond 2LPT. After publication of the main paper, Chan (2014) analyzed the non-linear evolution of Ψ , splitting it into its scalar and vector parts (the so-called “Helmholtz decomposition”). Looking at two-point statistics, he found that shell-crossing leads to a suppression of small-scale power in the scalar part, and, subdominantly, to the generation of a vector contribution.

Let $\psi(\mathbf{q}) \equiv \nabla_{\mathbf{q}} \cdot \Psi(\mathbf{q})$ denote the divergence of the displacement field, where $\nabla_{\mathbf{q}}$ is the divergence operator in Lagrangian coordinates. ψ quantifies the angle-averaged spatial-stretching of the Lagrangian dark matter “sheet” in comoving coordinates (Neyrinck, 2013). Let $\mathcal{P}_{\psi, \text{LPT}}$ and $\mathcal{P}_{\psi, \text{Nbody}}$ be the one-point probability distribution functions for the divergence of the displacement field in

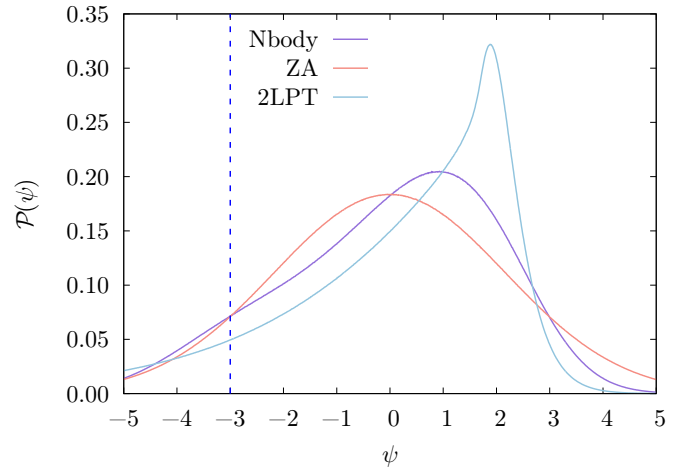


FIG. 1. Redshift-zero probability distribution function for the divergence of the displacement field ψ , computed from eight 1024 Mpc/ h -box simulations of 512^3 particles. A quantitative analysis of the deviation from Gaussianity of these PDFs is given in table I. The particle distribution is determined using: a full N -body simulation (purple curve), the Zel’dovich approximation (ZA, light red curve) and second-order Lagrangian perturbation theory (2LPT, light blue curve). The vertical line at $\psi = -3$ represents the collapse barrier about which ψ values bob around after gravitational collapse. A bump at this value is visible with full gravity, but LPT is unable to reproduce this feature. This regime corresponds to virialized, overdense clusters.

LPT and in N -body fields, respectively. We denote by \mathcal{P}_{δ} the corresponding PDFs for the Eulerian density contrast.

In figure 1, we show the PDFs of ψ for the ZA, 2LPT and full N -body gravity. The most important feature of ψ is that, whatever the model for structure formation, the PDF exhibits reduced non-Gaussianity compared to the PDF for the density contrast δ (see the upper panel

^{a)}Electronic mail: florent.leclercq@polytechnique.org

Model	\mathcal{P}_δ	\mathcal{P}_ψ
Skewness γ_1		
ZA	2.36 ± 0.01	-0.0067 ± 0.0001
2LPT	2.83 ± 0.01	-1.5750 ± 0.0002
N -body	5.14 ± 0.05	-0.4274 ± 0.0001
Excess kurtosis γ_2		
ZA	9.95 ± 0.09	$-2.2154 \times 10^{-6} \pm 0.0003$
2LPT	13.91 ± 0.15	3.544 ± 0.0011
N -body	62.60 ± 2.75	-0.2778 ± 0.0004

TABLE I. Non-Gaussianity parameters (the skewness γ_1 and the excess kurtosis γ_2) of the redshift-zero probability distribution functions \mathcal{P}_δ and \mathcal{P}_ψ of the density contrast δ and the divergence of the displacement field ψ , respectively. The confidence intervals given correspond to the $1\text{-}\sigma$ standard deviations among eight realizations. In all cases, γ_1 and γ_2 are reduced when measured from ψ instead of δ .

of figure 7 in [Leclercq et al., 2013](#), for comparison). The main reason is that \mathcal{P}_δ , unlike \mathcal{P}_ψ , is tied down to zero at $\delta = -1$. It is highly non-Gaussian in the final conditions, both in N -body simulations and in approximations to the true dynamics. For a quantitative analysis, we looked at the first and second-order non-Gaussianity statistics: the skewness γ_1 and the excess kurtosis γ_2 ,

$$\gamma_1 \equiv \frac{\mu_3}{\sigma^3} \quad \text{and} \quad \gamma_2 \equiv \frac{\mu_4}{\sigma^4} - 3, \quad (2)$$

where μ_n is the n -th moment about the mean and σ is the standard deviation. We estimated γ_1 and γ_2 at redshift zero in our simulations, in the one-point statistics of the density contrast δ and of the divergence of the displacement field ψ . The results are shown in table I. In all cases, we found that both γ_1 and γ_2 are much smaller when measured from \mathcal{P}_ψ instead of \mathcal{P}_δ .

At linear order in Lagrangian perturbation theory (the Zel’dovich approximation), the divergence of the displacement field is proportional to the density contrast in the initial conditions, $\delta(\mathbf{q})$, scaling with the negative growth factor, $-D_1(\tau)$:

$$\psi^{(1)}(\mathbf{q}, \tau) = \nabla_{\mathbf{q}} \cdot \Psi^{(1)}(\mathbf{q}, \tau) = -D_1(\tau)\delta(\mathbf{q}). \quad (3)$$

Since we take Gaussian initial conditions, the PDF for ψ is Gaussian at any time with the ZA. In full gravity, non-linear evolution slightly breaks Gaussianity. $\mathcal{P}_{\psi, N\text{-body}}$ is slightly skewed towards negative values while its mode gets shifted around $\psi \approx 1$. Taking into account non-local effects, 2LPT tries to get closer to the shape observed in N -body simulations, but the correct skewness is overshoot and the PDF is exceedingly peaked.

Figure 2 shows a slice of the divergence of the displacement field, measured at redshift zero for particles occupying a flat 512^2 -pixel Lagrangian sheet from one of our simulations. For comparison, see also the figures in [Mohayaee et al. \(2006\)](#); [Pueblas & Scoccimarro \(2009\)](#); [Neyrinck \(2013\)](#). We used the color scheme of the latter

paper, suggesting a topographical analogy when working in Lagrangian coordinates. As structures take shape, ψ departs from its initial value; it takes positive values in underdensities and negative values in overdensities. The shape of voids (the “mountains”) is found to be reasonably similar in LPT and in the N -body simulation. For this reason, the influence of late-time non-linear effects in voids is milder as compared to overdense structures, which makes them easier to relate to the initial conditions. However, in overdense regions where ψ decreases, it is not allowed to take arbitrary values: where gravitational collapse occurs, “lakes” form and ψ gets stuck around a collapse barrier, $\psi \approx -3$. As expected, these “lakes”, corresponding to virialized clusters, can only be found in N -body simulations, since LPT fails to accurately describe the highly non-linear physics involved. A small bump at $\psi = -3$ is visible in $\mathcal{P}_{\psi, N\text{-body}}$ (see figure 1). We checked that this bump gets more visible in higher mass-resolution simulations (200 Mpc/h box for 256^3 particles), where matter is more clustered. This means that part of the information about gravitational clustering can be found in the one-point statistics of ψ . Of course, the complete description of halos requires to precisely account for the shape of the “lakes”, which can only be done via higher-order correlation functions. More generally, it is possible to use Lagrangian information in order to classify structures of the cosmic web. In particular, DIVA ([Lavaux & Wandelt, 2010](#)) uses the shear of the displacement field and ORIGAMI ([Falck, Neyrinck & Szalay, 2012](#)) the number of phase-space folds. As pointed out by [Falck & Neyrinck \(2015\)](#), while these techniques cannot be straightforwardly used for the analysis of galaxy surveys, where we lack Lagrangian information, recently proposed techniques for physical inference of the initial conditions ([Jasche & Wandelt, 2013](#); [Jasche, Leclercq & Wandelt, 2015](#)) should allow their use with observational data.

Figure 3 shows two-dimensional histograms comparing N -body simulations to the LPT realizations for the density contrast δ and the divergence of the displacement field ψ . At this point, it is useful to note that a good mapping exists in the case where the relation shown is monotonic and the scatter is narrow. As pointed out by [Sahni & Shandarin \(1996\)](#) and [Neyrinck \(2013\)](#), matter in the substructure of 2LPT-voids has incorrect statistical properties: there are overdense particles in the low density region of the 2LPT δ -scatter plot. This degeneracy is also visible in the $\psi > 0$ region of the 2LPT ψ -scatter plot. On average, the scatter is bigger with ψ than with δ , in particular in overdensities ($\psi < 0$), since with LPT, particles do not cluster: ψ takes any value between 2 and -3 where it should remain around -3 .

Summing up our discussions in this addendum, we analyzed the relative merits of the Lagrangian divergence of the displacement field ψ , and the Eulerian density contrast δ at the level of one-point statistics. The important differences are the following:

1. Ψ being irrotational up to order two, its divergence

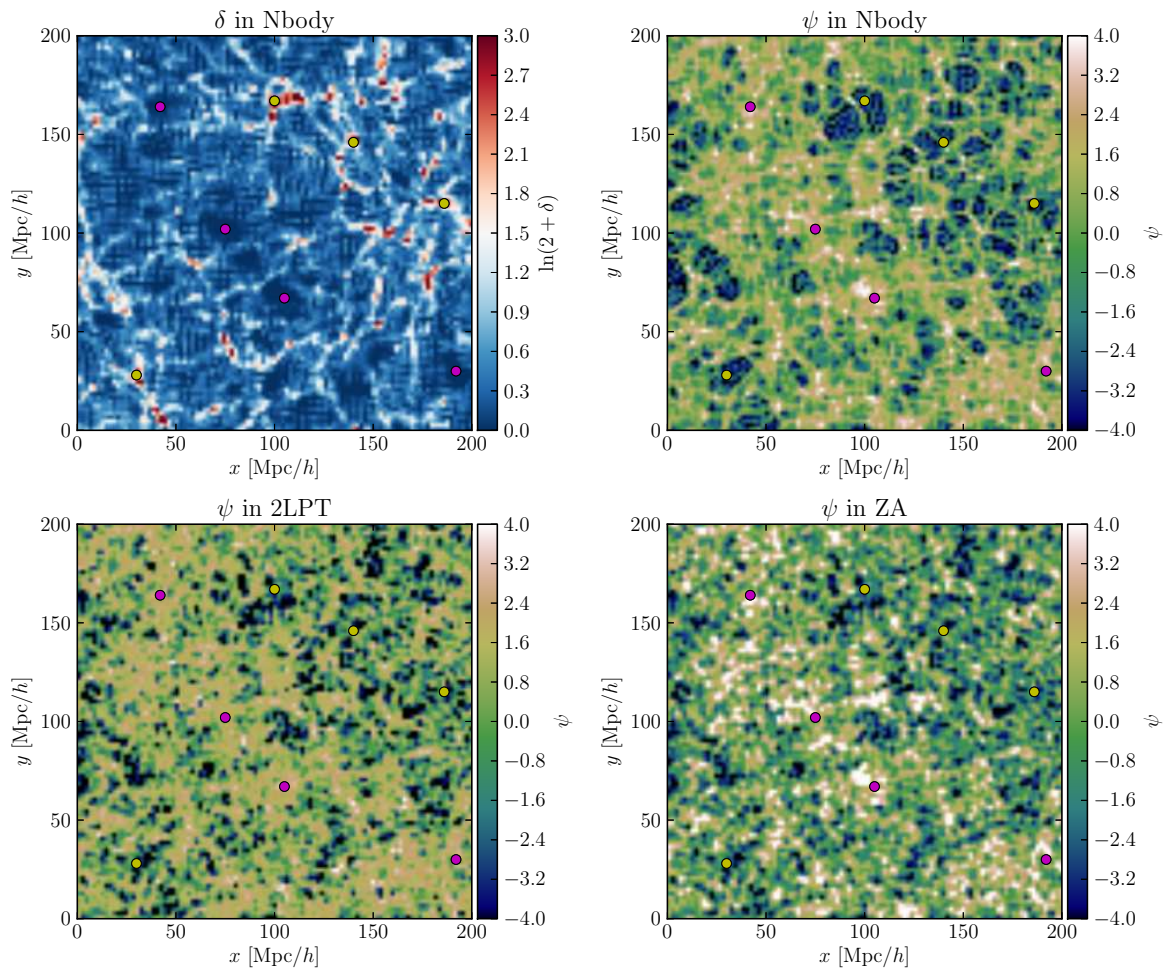


FIG. 2. Slices of the divergence of the displacement field, ψ , on a Lagrangian sheet of 512^2 particles from a 512^3 -particle simulation of box size $1024 \text{ Mpc}/h$, run to redshift zero. For clarity we show only a $200 \text{ Mpc}/h$ region. Each pixel corresponds to a particle. The particle distribution is determined using respectively a full N -body simulation, the Zel’dovich approximation (ZA) and second-order Lagrangian perturbation theory (2LPT). In the upper left panel, the density contrast δ in the N -body simulation is shown, after binning on a 512^3 -voxel grid. To guide the eye, some clusters and voids are identified by yellow and purple dots, respectively. The “lakes”, Lagrangian regions that have collapsed to form halos, are only visible in the N -body simulation, while the “mountains”, Lagrangian regions corresponding to cosmic voids, are well reproduced by LPT.

ψ contains nearly all information on the displacement field in one dimension, instead of three. The collapse barrier at $\psi = -3$ is visible in \mathcal{P}_ψ for N -body simulations but not for LPT. A part of the information about non-linear gravitational clustering is therefore encoded in the one-point statistics of ψ .

2. ψ exhibits much fewer gravitationally-induced non-Gaussian features than δ in the final conditions (figure 1 and table I).
3. However, the values of ψ are more scattered than the values of δ with respect to the true dynamics (figure 3), meaning that an unambiguous mapping is more difficult.

Note added. While this addendum was being refereed,

the work of Neyrinck (2015) appeared. It uses the spherical collapse prescription for ψ while checking various scales for the initial density field. The result is a fast scheme for producing approximate particle realizations.

- (Bernardeau, 1994) F. Bernardeau, *The nonlinear evolution of rare events*, *Astrophys. J.* **427**, 51 (1994), astro-ph/9311066.
- (Bernardeau et al., 2002) F. Bernardeau, S. Colombi, E. Gaztañaga, R. Scoccimarro, *Large-scale structure of the Universe and cosmological perturbation theory*, *Physics Reports* **367**, 1 (2002), astro-ph/0112551.
- (Bouchet et al., 1995) F. R. Bouchet, S. Colombi, E. Hivon, R. Juszkiewicz, *Perturbative Lagrangian approach to gravitational instability*, *Astron. & Astrophys.* **296**, 575 (1995), astro-ph/9406013.
- (Chan, 2014) K. C. Chan, *Helmholtz decomposition of the Lagrangian displacement*, *Phys. Rev. D* **89**, 083515 (2014), arXiv:1309.2243.

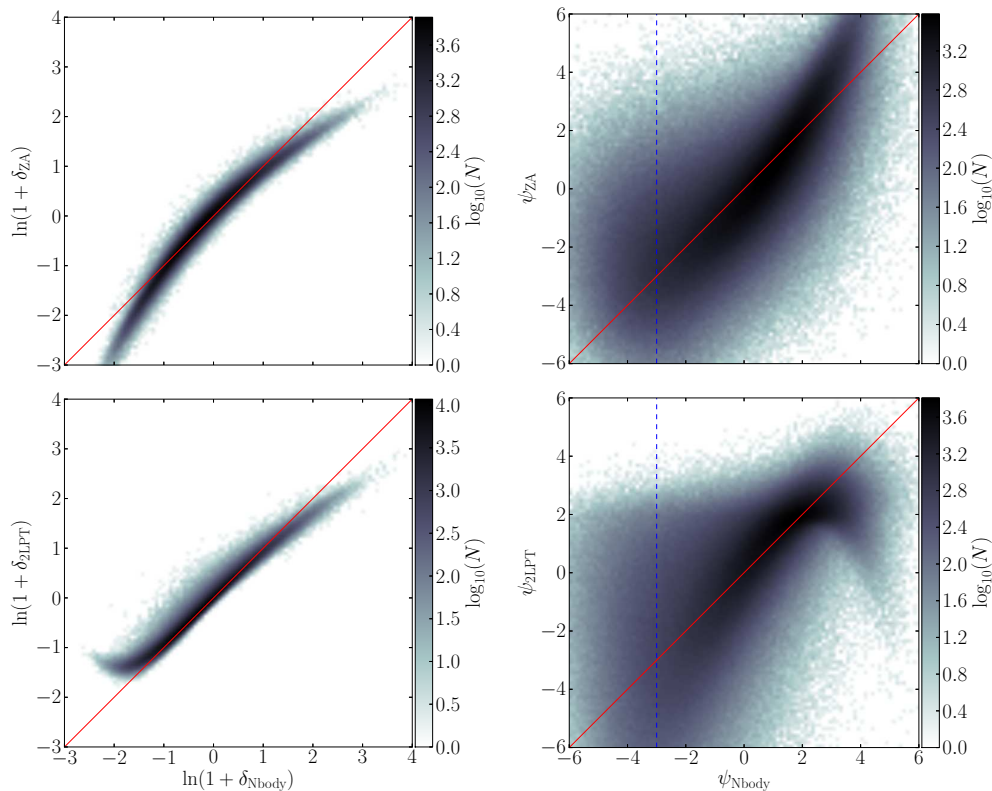


FIG. 3. *Left panel.* Two-dimensional histograms comparing particle densities evolved with full N -body dynamics (the x -axis) to densities in the LPT-evolved particle distributions (the y -axis). The red lines show the ideal $y = x$ locus. A turn-up at low densities is visible with 2LPT, meaning that some overdense regions are predicted where there should be deep voids. *Right panel.* Same plot for the divergence of the displacement field ψ . Negative ψ corresponds to overdensities and positive ψ correspond to underdensities. The dotted blue line shows the collapse barrier at $\psi = -3$ where particle get clustered in full gravity. The scatter is bigger with ψ than with δ , in particular in overdensities, since with LPT, particles do not cluster. The turn-up at low densities with 2LPT, observed with the density contrast, is also visible with the divergence of the displacement field.

- (Falck & Neyrinck, 2015) B. Falck, M. C. Neyrinck, *The persistent percolation of single-stream voids*, Mon. Not. R. Astron. Soc. **450**, 3239 (2015), arXiv:1410.4751.
- (Falck, Neyrinck & Szalay, 2012) B. L. Falck, M. C. Neyrinck, A. S. Szalay, *ORIGAMI: Delineating Halos Using Phase-space Folds*, Astrophys. J. **754**, 126 (2012), arXiv:1201.2353 [astro-ph.CO].
- (Jasche, Leclercq & Wandelt, 2015) J. Jasche, F. Leclercq, B. D. Wandelt, *Past and present cosmic structure in the SDSS DR7 main sample*, Journal of Cosmology and Astroparticle Physics **1**, 036 (2015), arXiv:1409.6308.
- (Jasche & Wandelt, 2013) J. Jasche, B. D. Wandelt, *Bayesian physical reconstruction of initial conditions from large-scale structure surveys*, Mon. Not. R. Astron. Soc. **432**, 894 (2013), arXiv:1203.3639 [astro-ph.CO].
- (Lavaux & Wandelt, 2010) G. Lavaux, B. D. Wandelt, *Precision cosmology with voids: definition, methods, dynamics*, Mon. Not. R. Astron. Soc. **403**, 1392 (2010), arXiv:0906.4101 [astro-ph.CO].
- (Leclercq et al., 2013) F. Leclercq, J. Jasche, H. Gil-Marín, B. Wandelt, *One-point remapping of Lagrangian perturbation theory*

- in the mildly non-linear regime of cosmic structure formation*, Journal of Cosmology and Astroparticle Physics **11**, 048 (2013), arXiv:1305.4642 [astro-ph.CO].
- (Mohayaee et al., 2006) R. Mohayaee, H. Mathis, S. Colombi, J. Silk, *Reconstruction of primordial density fields*, Mon. Not. R. Astron. Soc. **365**, 939 (2006), astro-ph/0501217.
- (Neyrinck, 2013) M. C. Neyrinck, *Quantifying distortions of the Lagrangian dark-matter mesh in cosmology*, Mon. Not. R. Astron. Soc. **428**, 141 (2013), arXiv:1204.1326 [astro-ph.CO].
- (Neyrinck, 2015) M. C. Neyrinck, *Truthing the stretch: Non-perturbative cosmological realizations with multiscale spherical collapse*, ArXiv e-prints (2015), arXiv:1503.07534.
- (Pueblas & Scoccimarro, 2009) S. Pueblas, R. Scoccimarro, *Generation of vorticity and velocity dispersion by orbit crossing*, Phys. Rev. D **80**, 043504 (2009), arXiv:0809.4606.
- (Sahni & Shandarin, 1996) V. Sahni, S. Shandarin, *Accuracy of Lagrangian approximations in voids*, Mon. Not. R. Astron. Soc. **282**, 641 (1996), astro-ph/9510142.